Microstructural Influence on Hydrogen Embrittlement in Advanced High-Strength Steels

PURDUE UNIVERSITY

Materials Engineering

Matt Clary, Sam Cleveland, Lisette Lopez Contreras, Mitch Parker
Faculty Advisors: Dr. David Johnson and Dr. Maria Okuniewski
Industrial Sponsors: Dr. Rongjie Song

The effects of hydrogen embrittlement were examined in martensitic (M) and dual phase (DP) advanced high strength steels via several mechanical and characterization tests after artificially charging them with hydrogen. Inclusion analysis showed that the martensitic samples had a greater area of inclusions within its microstructure, which were visible in the fracture surfaces. During tensile tests, the charged and uncharged dual phase and martensitic samples all reached a UTS and began necking before fracture, but both charged samples showed less thickness reduction between the UTS and fracture. Positron annihilation also showed a greater effect of hydrogen charging in M; with the lifetime difference being 6.3 and 5.0 ps for $\tau 1$ and $\tau 2$ between charged M and uncharged M, respectively, while the DP differences were 4.4 and 4.5 ps for $\tau 1$ and $\tau 2$, respectively. This indicated an increase in trapping site volumes within the martensite sample

This work is sponsored by
ArcelorMittal USA
East Chicago, IN

ArcelorMittal

Project Background

The automotive steel industry has a rapidly increasing demand for strong and lightweight steel at low cost for use in the structural and reinforcing components of the vehicle frame. Advanced high strength steels (AHSS) are a perfect candidate for this application. Unfortunately, AHSS are highly susceptible to hydrogen embrittlement, a process where hydrogen from the environment diffuses into a material's microstructure causing premature crack propagation and a decrease in ductility. In this project, ArcelorMittal's martensitic M1100 and dual-phase DP1180 AHSS (seen in Figure 1) were analyzed.

Table 1: Chemical compositions of ArcelorMittal's M1100 and DP1180 AHSS

Material	C	Mn	Si	Fe
M1100	0.12	0.45	-	Balance
DP1180	0.18	2.4	0.60	Balance

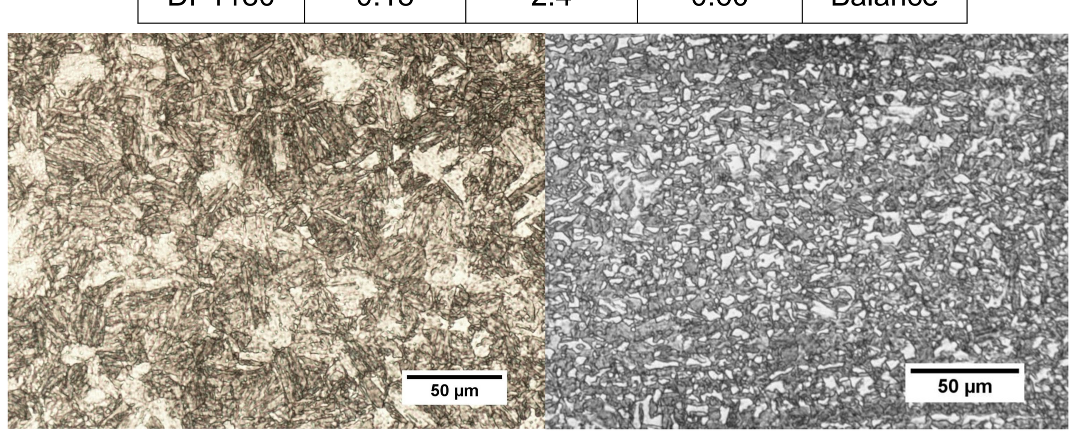

Figure 1: Chemical compositions (all in wt%) and microstructure images of M1100 (left) and dual phase DP1180 (right) advanced high strength steels.

Project Goal: The goal of this project was to use various characterization and mechanical tests to determine which material is less susceptible to hydrogen embrittlement.

Artificial Hydrogen Embrittlement

Atomic Hydrogen Charging: Hydrogen embrittlement can be simulated through artificially causing hydrogen diffusion via an electrolytic cell. A current of 10mA is passed through an acidic solution with the steel sample as the cathode. This caused the hydrogen to dissociate at the surface and diffuse into the sample due to the concentration gradient. The tensile dogbones (gauge length: 80x12x2 mm) and the smaller coupons (25x25x2 mm) were charged for one hour.

Figure 2: Hydrogen charging apparatus used for this project

Thermal Desorption Analysis: Thermal Desorption Analysis (TDA) was used to measure the amount of hydrogen trapped within the microstructure of the steel samples. Three DP and three M samples were tested at ArcelorMittal and each had a minimum of 0.60 ppm diffusible hydrogen when heated to 250 ℃. This proved that the charging method was functional.

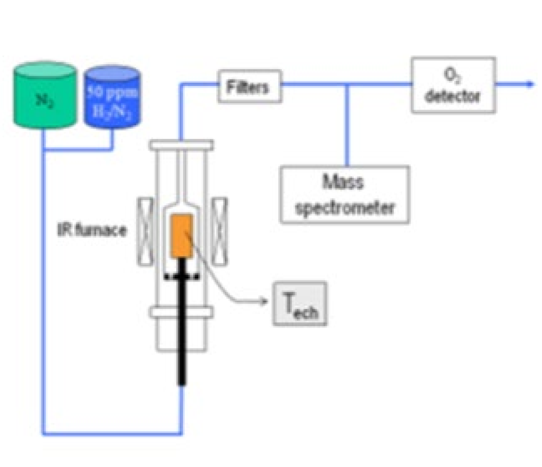

Figure 3: An overview of the TDA process. Acquired from ArcelorMittal.

Automated Steel Cleanliness Analysis Tool (ASCAT)

ASCAT is used to measure the types, amount, and size of inclusions within steel samples. Inclusions can act as hydrogen trapping sites and increase the solubility of hydrogen into the sample, thereby increasing susceptibility to hydrogen embrittlement.

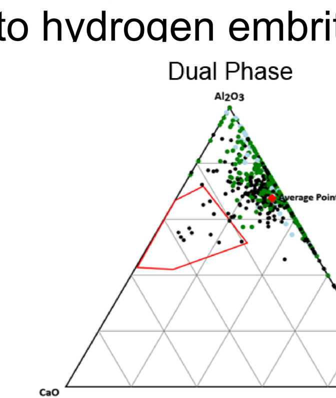

Material	Total Oxide (Area %)	Total Oxide Count
Dual Phase	1.7E-04	1008
Martensite	2.8E-04	871

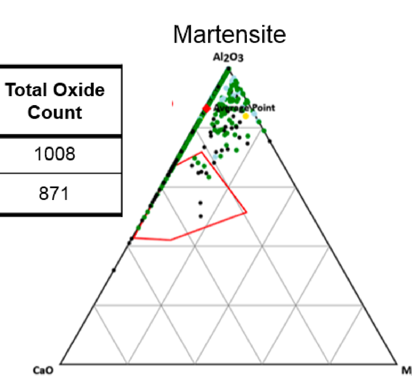

Figure 5: Ternary phase displaying oxide distribution, size, and phase in dual phase and martensite sample. The red lines on the diagram display the liquidus region for the oxides.

The martensitic steels showed a higher content of Al_2O_3, a lower total inclusion count, but a greater total oxide area. The lower inclusion count was consistent with the ASTM-45 results. The greater total oxide area shown by the martensitic steels can be attributed to the generally larger size of the inclusions when compared to the smaller inclusions within the dual-phase steels. The larger oxide area provides more locations where hydrogen can diffuse into, become trapped, and eventually embrittle the steel.

Positron Annihilation (PALS)

Positron Annihilation Lifetime Spectroscopy is a used to determine the defect density near the surface of a material. The detectors for PALS measure the time between implantation and annihilation of positrons.

Table 3: Positron lifetime in uncharged and charged M and DP samples. Change in lifetime is the increase of tau from uncharged to charged.

Material	Lifetime (ps)		Change in Lifetime (ps)	
	$\tau 1$	$\tau 2$	$\tau 1$	$\tau 2$
Uncharged M	132.0	371.3	6.3	5.0
Charged M	138.3	376.3		
Uncharged DP	145.5	390.6	4.4	4.5
Charged DP	147.9	395.1		

Lifetime $\tau 1$ is characteristic of annihilation in the standard lattice. Lifetime $\tau 2$ is annihilation vacancies and other defects. An increase in $\tau 1$ means that hydrogen has caused the lattice to expand. An increase in $\tau 2$ demonstrates an increase in the size of larger open-volume defects. Since the change in $\tau 1$ and $\tau 2$ for martensite was greater than in dual phase (martensite and ferrite), it can be assumed that martensitic steel is more affected by hydrogen.

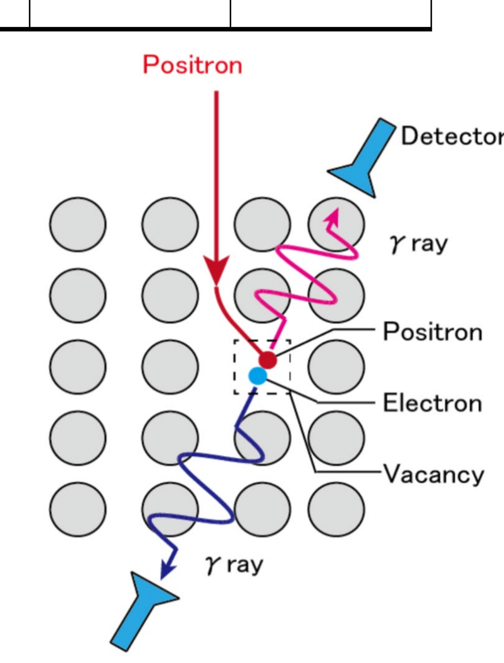

Figure 6: A schematic of a positron-electron interaction (annihilation) within a vacancy and the produced gamma rays going to the detectors [2].

[2] Retrieved from: Uedono, A., Study of dynamics of carrier trapping/scattering in singularity crystal structure by means of positron annihilation

Tensile Testing & Fracture Surface

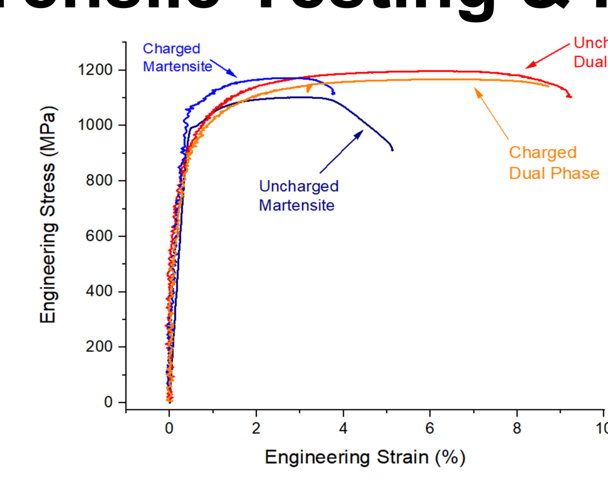

Figure 7 (left): Tensile data for each sample until extensometer was removed after UTS

Table 4: Mechanical properties of charged and uncharged M and DP

Material	YS (MPa)	UTS (MPa)	Uniform Elongation (%)
Uncharged M	1010	1100	2.9
Uncharged DP	980	1200	6.0
Charged M	1090	1170	2.6
Charged DP	960	1170	6.3

The hydrogen charged samples did not affect the ductility before the UTS, but the difference in gauge thickness reduction as seen below in Figure 8 indicates that more necking occurred in the uncharged samples after the UTS.

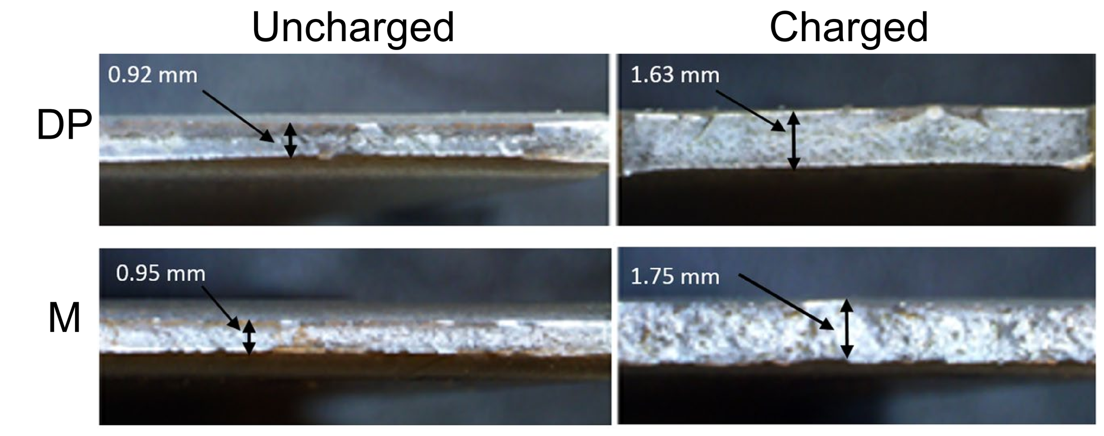

Figure 8: Optical images of the gauge thickness reduction after tensile testing. The charged samples showed less thickness reduction under stress

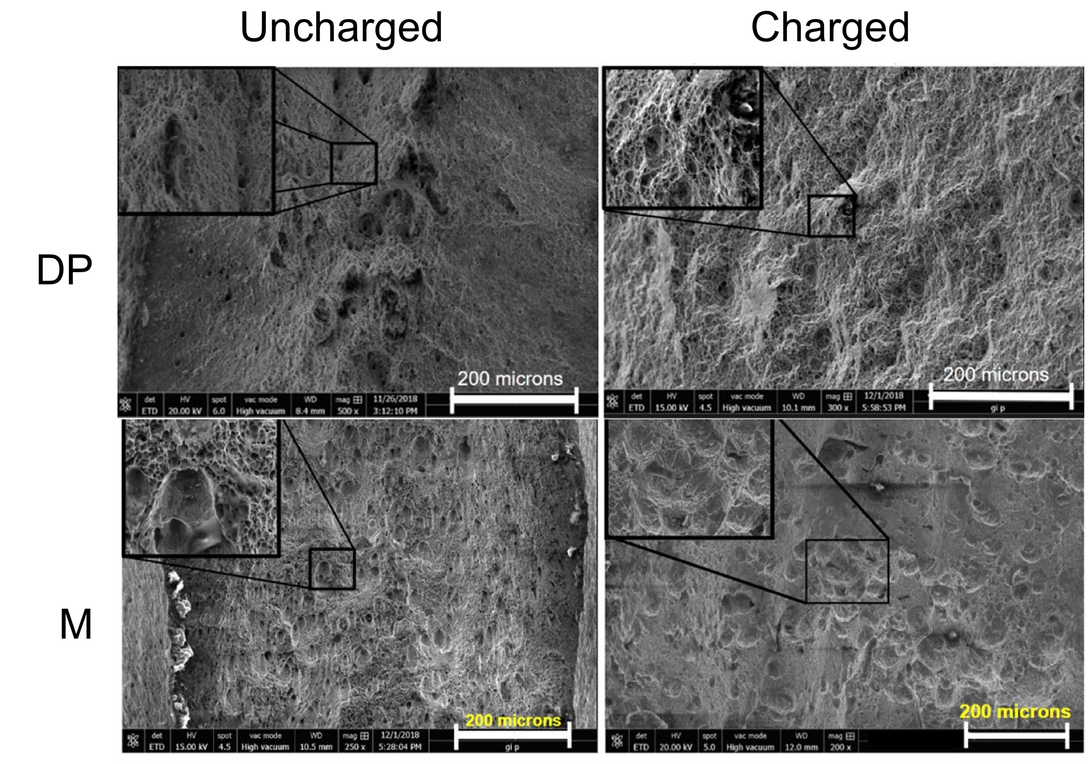

Figure 9: SEM images of the fracture surfaces of the tensile tested samples.

The fracture surface in Figure 9 provided evidence of ductile fracture by microvoid coalescence in all samples, where the microvoids were created after the UTS. The large voids visible in the images were associated with large inclusions.

Acknowledgments

Special thanks to: Nelyan Lopez-Perez (PALS), Duo Huang (tensile), Jonova Thomas (SEM), Dr. Jonathan Shannahan and his students (sample storage), and the ArcelorMittal team (ASCAT & TDA) for their assistance in this project.

ASTM E45

ASTM E45 allows for a simple evaluation of inclusions to determine the cleanliness of the steel. The results show the presence of nitride inclusions. Elements such as Ti, Zr, and Fe form a stable compound with nitrogen. FeN is an especially undesirable inclusion because it causes precipitation of fine dispersed non-metallic particles along grain boundaries which weaken the bonding of grains, reducing the plasticity[1]. The dual phase steel presented a higher number of these inclusions.

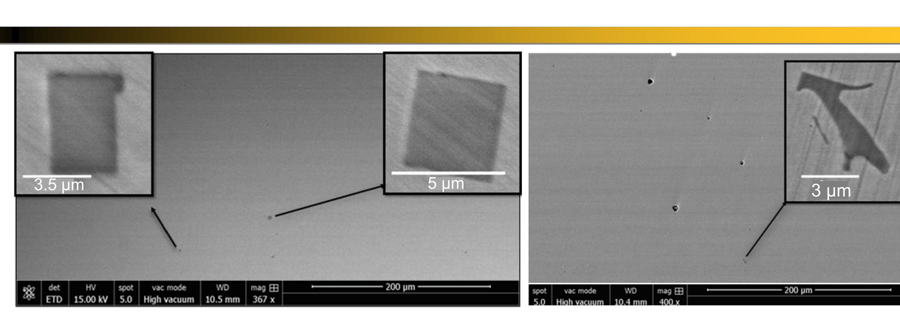

Figure 4: SEM images of inclusions in the martensitic steel (right) and dual phase steel (left)

Table 2: Size and quantity of Ti, N, and Fe - based inclusions in each sample and the number of pores found

Material	Main Elements	# of Inclusions	Average Radius	Radius Deviation	# of Pull outs/Pores
DP	Ti, N, Fe	28	0.31µm	0.08	87
M	Ti, N, Fe	18	0.66µm	0.42	78

Conclusions

Based on the fracture surface microscopy, it is evident that both samples were embrittled by hydrogen. While it is challenging to quantify how much the samples were embrittled from these images, the PALS data showed that the martensitic steel was more affected by hydrogen embrittlement based on positron lifetime differences. One possible explanation is that the martensitic steel had a greater area of inclusions, according to the ASCAT and ASTM E45 results. A greater number of inclusions, especially oxides, meant that there were a greater number of irreversible hydrogen trapping sites.

In conclusion, the data showed that both the martensitic and dual phase AHSS samples were affected by hydrogen embrittlement after the materials' ultimate tensile strengths; however, according to PALS data, the dual phase steel was less susceptible.

Reference: [1] Bizyukov, Pavel, "An experimental study of non-metallic inclusions precipitation and its effect on impact toughness variations in low alloy steel subjected to complex deoxidation" (2017). Electronic Theses and Dissertations. pg 368.